

Hygro-Thermal Effects on Stress Analysis of Tapered Laminated Composite Beam

Debabrata Gayen, Tarapada Roy*

Department of Mechanical Engineering, National Institute of Technology Rourkela, Rourkela, 769008, India

Abstract The present work deals with an analytical method in order to determine the stress distributions (such as axial in-plane stresses and inter-laminar shear stresses) in multilayered symmetric and anti-symmetric circular tapered laminated composite beams under hygro and thermal loadings. In the present analysis, all derivations for calculation of stresses have been developed based on the modification of conventional lamination and parallel axis theories. The hygro-thermal loads are considered as a linear function of coordinates in the planes of each layer. Hygro-thermally induced stresses are obtained for various types of laminates with cantilevered boundary conditions at different moisture concentrations and temperatures. A complete code has been developed using MATLAB program and validation of the present formulations has been done by comparison with available solutions in the literature. Various results have also been found for tapered laminated cantilever beams of carbon/epoxy and graphite/epoxy materials. It has been observed that effects of stacking sequence, fiber orientation, coefficient of thermal expansion (CTE) and coefficient of moisture expansion (CME) have significance roles in the change of inter-laminar shear and axial in-plane stresses distribution through the laminate thickness.

Keywords Tapered laminated composite, Conventional lamination theory, laminated plate approach, Inter-laminar shear stresses, axial in-plane stresses, Hygro-thermal load

1. Introduction

Laminated composite structures/systems are increasingly used in aerospace and other engineering applications due to their high specific strength, stiffness and good corrosion resistance, low coefficients of thermal expansion and of hygro-thermal expansion. They are subjected to different environmental conditions during service life. It has been seen that moisture and temperature have an adverse effect on the performance of composites (viz. stiffness and strength are reduced with the increase in moisture concentration and temperature). Although due to thermal expansion mismatch between layers of different fiber orientations, thermal stresses induced within and between laminas and thermal behaviors of the laminated composite material are more pronounced than that of isotropic materials. Accurate evaluation of bending stiffness is an important factor for better prediction of axial in-plane stresses, inter-laminar shear stresses and deflection, bulking and vibration responses of structures. Some of the important works in the directions are presented in the following paragraph.

Whitney and Ashton[1] considered the effect of environment on the bending of symmetric and un-symmetric

laminated composite plates. Pipes et al.[2] analyzed the stresses in laminated composite plates subjected to the combined effect of elevated temperature and absorbed moisture. Sims and Wilson[3] derived an approximate elasticity solution for the transverse shearing stresses in a multilayered anisotropic composite beam. Sai Ram and Sinha[4] presented the effects of moisture and temperature on the bending characteristics of laminated composite plates using finite element method (FEM). Sai Ram and Sinha[5] investigated the effects of moisture and temperature on the free vibration of laminated composite plates. Sai Ram and Sinha [6] also investigated the effect of moisture and temperature on the buckling analysis of laminated composite plates. Chanand Demirhan[7] developed two analytical closed-form solutions, such as laminated plate approach and laminated shell approach, to evaluate the stiffness matrices and bending stiffness of the laminated composite circular tube. Tam and Wang[8] presented a state space approach for the analysis of extension, torsion, bending, shearing and pressuring of laminated composite tube. Patel et al.[9] presented the static and dynamic characteristics of thick composite laminates exposed to hygro-thermal environments using eight-noded C^0 isoparametric higher order quadrilateral plate elements. Zenkour[10] investigated the static thermo-elastic response of symmetric and anti-symmetric cross-ply laminated plates considering unified shear deformation plate theory. Naidu and Sinha[11] analyzed the large deflection bending behaviour of laminated composite

* Corresponding author:

tarapada@nitrrkl.ac.in (Tarapada Roy)

Published online at <http://journal.sapub.org/cmaterials>

Copyright © 2013 Scientific & Academic Publishing. All Rights Reserved

cylindrical shell panels subjected to hygro-thermal environments using FEM. Wang et al.[12] studied hygro-thermal effect on the response of dynamic inter-laminar stresses distribution in laminated plates with piezoelectric actuator layers. Naidu and Sinha[13] analyzed free vibration behaviour of laminated composite shell subjected to hygro-thermal environments using FEM. Bahrami and Nosier[14] employed the displacement fields of general cross-ply, symmetric, and anti-symmetric angle-ply laminates under thermal and hygroscopic loadings and developed elasticity based solution for predicting the inter-laminar normal and shear stress distributions. Su[15] developed closed-form analytical solutions for evaluating the thermal induced stresses in laminated composite tubular and rectangular beams. Rao[16] developed closed-form expressions based on modifying the laminated plate approach to determine the displacement and twisting angle of tapered composite tube under axial tension and torsion. Shao and Ma[17] carried out the thermo-mechanical analysis of functionally graded hollow circular cylinders subjected to mechanical loads and linearly increasing boundary temperature. Syed et al.[18] presented the analytical expressions for computing thermal stresses in fiber reinforced composite beam with rectangular and hat sections under uniform temperature environment. Zenkour[19] studied the hygro-thermal bending analysis of functionally graded plate resting on elastic foundations. Singh and Chakrabarti[20] carried out hygro-thermal analysis of laminated composite plates using an efficient higher order shear deformation theory. Here plate model implemented with a computationally efficient C^0 finite element using consistent strain field.

Although literature review revealed that a lot of research work has been done on the inter-laminar shear stresses distribution and axial in-plane stress distribution analysis of laminated composite structures and also it is still remain as important area on research. In the present work a tapered laminated composite beam model has been considered and the details analysis has been carried out under both hygro and thermal loadings.

2. Hygro-Thermo-Mechanical Analysis of a Tapered Laminated Composite Beam

In the present model, the cross-sectional plane of the beam remains plane after deformation.

2.1. Geometry of Tapered Laminated Composite Beam

A tapered laminated composite beam is considered with larger end radius R_L , smaller end radius R_S , Length L and a beam thickness t as shown in Fig. 1. The radius of the tapered beam at a distance x from the larger end, R_x will be expressed as $R_x = R_L - x \tan \alpha$. Where α is the taper angle

of the beam and $\tan \alpha = \frac{\Delta R}{L}$ and difference between the large and small radii of the beam is $\Delta R = R_L - R_S$.

2.2. Laminated Constitutive Equation

Composite laminate consists of a set of multiple layers stacking together with different fiber orientations. It is very importance to analyze this problem based on layer by layer analysis. To circumvent or encompass this tedious approach, the laminate is often analyzed based upon its mid-plane axes as a reference axis. The properties of each layer are transformed to the reference axis. Now the general load-deformation relation of laminate composite is given as

$$\begin{bmatrix} \bar{N} \\ \bar{M} \end{bmatrix} = \begin{bmatrix} N \\ M \end{bmatrix} + \begin{bmatrix} N^{HT} \\ M^{HT} \end{bmatrix} = \begin{bmatrix} A & B \\ B & D \end{bmatrix} \begin{bmatrix} \varepsilon_0 \\ \kappa \end{bmatrix} \quad (1)$$

Where,

$$[N] = \sum_{i=1}^k \int_{z_k}^{z_{k+1}} [\sigma]^k . dz, [M] = \sum_{i=1}^k \int_{z_k}^{z_{k+1}} [\sigma]^k . z . dz \quad (2)$$

$$[N^{HT}] = \sum_{i=1}^k \int_{z_k}^{z_{k+1}} [\bar{Q}]^k \{ [\alpha]_{x,y}^k \Delta T + [\beta]_{x,y}^k \Delta C \} dz \quad (3)$$

$$[M^{HT}] = \sum_{i=1}^k \int_{z_k}^{z_{k+1}} [\bar{Q}]^k \{ [\alpha]_{x,y}^k \Delta T + [\beta]_{x,y}^k \Delta C \} z dz$$

$$[A] = \sum_{i=1}^k \int_{z_k}^{z_{k+1}} [\bar{Q}]^k dz, [B] = \sum_{i=1}^k \int_{z_k}^{z_{k+1}} [\bar{Q}]^k z dz \quad (4)$$

$$[D] = \sum_{i=1}^k \int_{z_k}^{z_{k+1}} [\bar{Q}]^k z^2 dz$$

In the above equation,

$[\varepsilon_0]$ and $[\kappa]$, $[\bar{N}]$ and $[\bar{M}]$, $[N]$ and $[M]$, $[N^{HT}]$ and $[M^{HT}]$ matrices are mid-plane strain and curvature, net resultant forces and moments, applied load and moment, hygro-thermal induced force and moment respectively.

$[A]$, $[B]$, $[D]$, $[\beta]_{x,y}^k$ and $[\alpha]_{x,y}^k$ matrices are in-plane or extensional stiffness, extensional-bending coupling stiffness, bending stiffness, coefficient of thermal expansion (CTE) and coefficient of moisture expansion (CME) of k^{th} ply in the laminate x - y coordinate system. Now ΔT and ΔC are the change of temperature and moisture concentration respectively. Here, z_k and z_{k+1} are the inner and outer coordinate of the k^{th} ply respectively.

Now, constitutive (i.e. stress-strain) relation for a lamina in the principal material directions are presented as follows,

$$\begin{bmatrix} \sigma_1 \\ \sigma_2 \\ \tau_{12} \end{bmatrix} = \begin{bmatrix} Q_{11} & Q_{12} & 0 \\ Q_{21} & Q_{22} & 0 \\ 0 & 0 & Q_{66} \end{bmatrix} \begin{bmatrix} \varepsilon_1 \\ \varepsilon_2 \\ \gamma_{12} \end{bmatrix} \quad (5)$$

Now reduced stiffness matrix $[Q]^k$ for k^{th} ply defined as,

$$\begin{aligned} Q_{11} &= \frac{E_1}{1-\nu_{12}\nu_{21}}, Q_{22} = \frac{E_2}{1-\nu_{12}\nu_{21}} \\ Q_{12} = Q_{21} &= \frac{\nu_{21}E_1}{1-\nu_{12}\nu_{21}} = \frac{\nu_{12}E_2}{1-\nu_{12}\nu_{21}} \\ Q_{66} &= G_{12} \end{aligned} \quad (6)$$

Where E_1, E_2, G_{12} and ν_{12} are the elastic moduli along longitudinal, transverse direction, shear modulus in 1-2 planes and Poisson's ratio along the principal material direction respectively.

2.3. In-Plane Stress Calculation

For hygro-thermal stress analysis of tapered laminated composite beam, laminated plate approach is chosen due to its simplicity. Laminated plate approach is derived based on the conventional lamination theory and translation of laminate axis. Here infinitesimal element, which is inclined an angle θ with respect to the axis of the beam, z is rotated about the x axis as shown in Fig. 1.

The total extensional, coupling and bending stiffness matrices of an n ply laminate with a ply thickness t_{ply} and mid-thickness radius of the tapered tube at a distance x from the larger end, R_x are obtained as follow

$$\begin{aligned} [\bar{A}]_{x,y} &= R_x \int_0^{2\pi} [A']_{x,y} d\theta = R_x \sum_{n=1}^k [\bar{Q}]_{x,y} (z'_{k+1} - z'_k) \\ [\bar{B}]_{x,y} &= R_x \int_0^{2\pi} [B']_{x,y} d\theta = \frac{1}{2} R_x \sum_{n=1}^k [\bar{Q}]_{x,y} (z'^2_{k+1} - z'^2_k) \\ [\bar{D}]_{x,y} &= R_x \int_0^{2\pi} [D']_{x,y} d\theta = \frac{1}{3} R_x \sum_{n=1}^k [\bar{Q}]_{x,y} (z'^3_{k+1} - z'^3_k) \end{aligned} \quad (7)$$

Where transformed reduced stiffness matrix of k^{th} ply $[\bar{Q}]_{x,y}^k$ is given in appendix. $[A']_{x,y}, [B']_{x,y}$ and $[D']_{x,y}$ can be

$$\begin{aligned} [A']_{x,y} &= [A]_{x,y} \\ [B']_{x,y} &= [B]_{x,y} + R_x \cos\theta [A]_{x,y} \\ [D']_{x,y} &= [D]_{x,y} + 2R_x \cos\theta [B]_{x,y} + (R_x \cos\theta)^2 [A]_{x,y} \end{aligned} \quad (8)$$

2.4. Determination of Hygro-thermal Force and Moment

For finding the hygro-thermal force and moment expression the following steps are followed. In $x-y$ coordinate system, CTE i.e. $[\alpha]_{x,y}^k$ and CME i.e. $[\beta]_{x,y}^k$ of

k^{th} ply of the composite beam are obtained from the transformation of CTE and CME of the lamina in 1-2 coordinate. Now from Fig. 1, these are first rotated about the x axis with an angle θ , rotated about z axis with the angle of fiber orientation $-\phi$. So the transformation of CTE and CME in $x-y$ coordinates system can be written as,

$$\begin{aligned} [\alpha]_{x,y}^k &= [T(-\phi)]_{\epsilon}^k [\alpha']_{1,2} = [T(-\phi)]_{\epsilon}^k [T(\theta)]_{\epsilon}^k [\alpha]_{1,2} \\ [\beta]_{x,y}^k &= [T(-\phi)]_{\epsilon}^k [\beta']_{1,2} = [T(-\phi)]_{\epsilon}^k [T(\theta)]_{\epsilon}^k [\beta]_{1,2} \end{aligned} \quad (9)$$

$[T]_{\epsilon}$ is given in appendix. The hygro-thermal induced force and moment are obtained by integrating thermal strain through the thickness of lamina, and can be expressed as,

$$\begin{aligned} [N]_{x,y}^{HT} &= \sum_{k=1}^n [\bar{Q}]_{1,2}^k \left\{ \Delta T [\alpha]_{x,y}^k + \Delta C [\beta]_{x,y}^k \right\}^T \{ z'_{k+1} - z'_k \} \\ [M]_{x,y}^{HT} &= \sum_{k=1}^n [\bar{Q}]_{1,2}^k \left\{ \frac{\Delta T}{2} [\alpha]_{x,y}^k + \frac{\Delta C}{2} [\beta]_{x,y}^k \right\}^T \{ z'^2_{k+1} - z'^2_k \} \end{aligned} \quad (10)$$

Where ΔT and ΔC are the difference of temperature and moisture content respectively. The forces and moments of the mid plane of the lamina obtained using equation (10) can be transformed as,

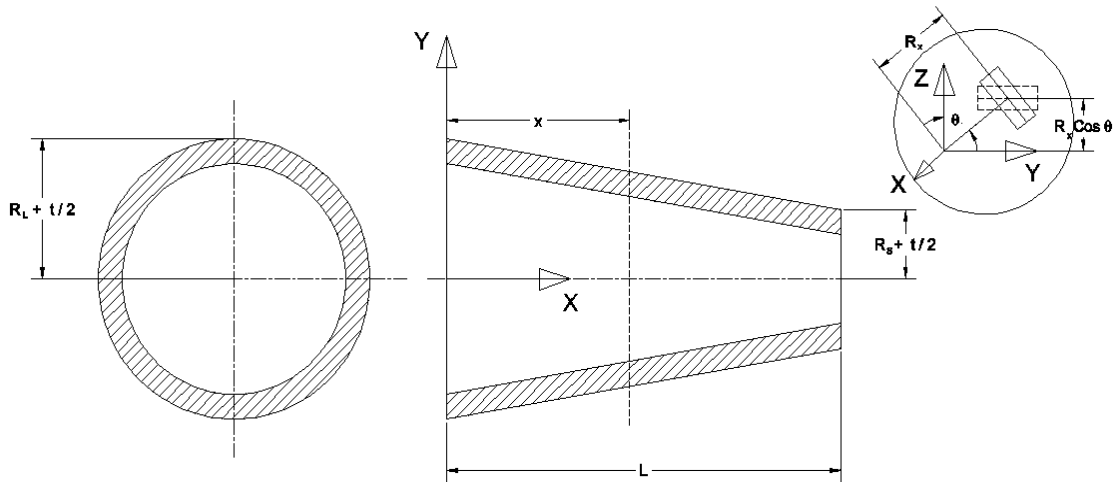


Figure 1. Geometry of the tapered laminated composite beam

$$\begin{aligned}
 [N]_{x,y}^{HT} &= \sum_{k=1}^n [\bar{Q}]_{1,2}^k \left\{ \Delta T [\alpha]_{x,y}^k + \Delta C [\beta]_{x,y}^k \right\}^T \\
 &\quad \left\{ (z'_{k+1} + R_x \cos \theta) - (z'_k + R_x \cos \theta) \right\} = [N]_{x',y'}^{HT} \\
 [M]_{x,y}^{HT} &= \sum_{k=1}^n [\bar{Q}]_{1,2}^k \left\{ \frac{\Delta T}{2} [\alpha]_{x,y}^k + \frac{\Delta T}{2} [\beta]_{x,y}^k \right\}^T \quad (11) \\
 &\quad \left\{ (z'_{k+1} + R_x \cos \theta)^2 - (z'_k + R_x \cos \theta)^2 \right\} \\
 &= [M]_{x',y'}^{HT} + R_x \cos \theta [N]_{x',y'}^{HT}
 \end{aligned}$$

The overall hygro-thermal induced force and moment can be expressed as,

$$[\bar{N}]_{x,y}^{HT} = \int_0^{2\pi} [N]_{x,y}^{HT} R_x d\theta, [\bar{M}]_{x,y}^{HT} = \int_0^{2\pi} [M]_{x,y}^{HT} R_x d\theta \quad (12)$$

The total ply strain at any point in the k^{th} ply of the laminate can be obtained by using the following relations

$$\begin{bmatrix} \epsilon_x^{Total} \\ \epsilon_y^{Total} \\ \gamma_{xy}^{Total} \end{bmatrix}^k = \begin{bmatrix} \epsilon_x^0 \\ \epsilon_y^0 \\ \gamma_{xy}^0 \end{bmatrix} + (R_x + z') \cos \theta \begin{bmatrix} \kappa_x \\ \kappa_y \\ \kappa_{xy} \end{bmatrix} \quad (13)$$

Where, $[\epsilon^{Total}]_{x,y}^k$, $[\epsilon^0]_{x,y}$ and $[\kappa]_{x,y}$ represent the total ply strain, mid-plane strain and mid-plane curvature respectively. The mechanical strain is obtained by subtracting the thermal strain from the total strain. Finally, the ply stress can be obtained by multiplying the matrix of the ply with the mechanical strain. It can be expressed as,

$$\begin{aligned}
 [\epsilon^{Total}]_{x,y}^k &= [\epsilon^0]_{x,y} + (R_x + z') \cos \theta [\kappa]_{x,y} \\
 [\epsilon^M]_{x,y}^k &= [\epsilon^{Total}]_{x,y}^k - [\alpha]_{x,y}^k \Delta T - [\beta]_{x,y}^k \Delta C \quad (14)
 \end{aligned}$$

So, axial in-plane stress equation will be

$$\begin{aligned}
 [\sigma]_{x,y}^k &= [\bar{Q}]_{x,y}^k [\epsilon^M]_{x,y}^k \\
 &= [\bar{Q}]_{x,y}^k \left\{ \begin{bmatrix} \epsilon_x^0 \\ \epsilon_y^0 \\ \gamma_{xy}^0 \end{bmatrix} + (R_x + z') \cos \theta [\kappa]_{x,y} \right. \\
 &\quad \left. - [\alpha]_{x,y}^k \Delta T - [\beta]_{x,y}^k \Delta C \right\} \quad (15)
 \end{aligned}$$

2.5. Inter-laminar Shear Stress Formulation under Transverse Load

Sims and Wilson[3] developed an analytical solution of the inter-laminar shear stresses of the laminated composite beam subjected to a transverse load q . For analytical solution, two assumptions are made in derivation and these are, stresses not depend on y direction and σ_z, τ_{yz} are small and can be neglected. So, the equations at equilibrium for the k^{th} layer of the laminate can be written as,

$$\begin{aligned}
 \frac{\partial \sigma_x^k}{\partial x} + \frac{\partial \tau_{xy}^k}{\partial y} + \frac{\partial \tau_{xz}^k}{\partial z} &= 0 \\
 \frac{\partial \tau_{xy}^k}{\partial x} + \frac{\partial \sigma_y^k}{\partial y} + \frac{\partial \tau_{yz}^k}{\partial z} &= 0 \\
 \frac{\partial \tau_{xz}^k}{\partial x} + \frac{\partial \tau_{yz}^k}{\partial y} + \frac{\partial \sigma_z^k}{\partial z} &= 0
 \end{aligned} \quad (16)$$

The lamina is assumed to be under plane stress condition (i.e. stresses $\sigma_z, \tau_{yz}, \tau_{xz}$ are assumed to be zero). Therefore, for finding the inter-laminar stress components beam is consider as narrow, so the stresses are assumed to be independent of y . For multi-layer laminate with $\tau_{xz}^0 = 0$, above equation (16) can be reduced as,

$$\tau_{xz}^k = - \sum_{i=1}^k \int_{z_i}^{z_{i+1}} \frac{\partial \sigma_x^i}{\partial x} dz \quad (17)$$

The laminated constitutive equation including hygro-thermal effect can be express as,

$$\begin{bmatrix} \epsilon^0 \\ \kappa \end{bmatrix}_{x,y} = \begin{bmatrix} a & b \\ b^T & d \end{bmatrix} \begin{bmatrix} N + N^{HT} \\ M + M^{HT} \end{bmatrix}_{x,y} \quad (18)$$

Where, $\begin{bmatrix} a & b \\ b^T & d \end{bmatrix} = \begin{bmatrix} A & B \\ B & D \end{bmatrix}^{-1}$

Hence, in the present analysis tapered cantilever beam is considered as a narrow beam, q is the transverse shear load per unit width and the in-plane forces are not considered on beam. So, $N_x = N_y = N_{xy} = M_y = M_{xy} = 0$ and $\frac{\partial M_x}{\partial x} = -q$.

After putting the equations (15) and (18) into equation (17), obtained the following expression

$$\tau_{xz}^k = - \sum_{i=1}^k \int_{z_k}^{z_{k+1}} \left\{ \begin{aligned} & \bar{Q}_{11}^i \left(\frac{\partial \epsilon_x^0}{\partial x} + (R_x + z_i) \cos \theta \frac{\partial \kappa_x}{\partial x} \right) \\ & + \bar{Q}_{12}^i \left(\frac{\partial \epsilon_y^0}{\partial x} + (R_x + z_i) \cos \theta \frac{\partial \kappa_y}{\partial x} \right) \\ & + \bar{Q}_{16}^i \left(\frac{\partial \gamma_{xy}^0}{\partial x} + (R_x + z_i) \cos \theta \frac{\partial \kappa_{xy}}{\partial x} \right) \end{aligned} \right\} dz \quad (19)$$

Since for the present case $[N^{HT}]$ and $[M^{HT}]$ not depend on x , hence, equation (19) becomes,

$$\begin{aligned}
 \tau_{xz}^k &= \sum_{i=1}^k \int_{z_k}^{z_{k+1}} \left\{ \begin{aligned} & \left(\bar{Q}_{11}^i b_{11} + \bar{Q}_{12}^i b_{12} + \bar{Q}_{16}^i b_{16} \right) \\ & + (R_x + z_i) \cos \theta \left(\bar{Q}_{11}^i d_{11} + \bar{Q}_{12}^i d_{12} + \bar{Q}_{16}^i d_{16} \right) \end{aligned} \right\} q dz \\
 \tau_{xz}^k &= \sum_{i=1}^k \int_{z_k}^{z_{k+1}} \left\{ \left[\bar{Q}^i \right]_{1,2} [B]_{1,2} + (R_x + z_i) \cos \theta \left[\bar{Q}^i \right]_{1,2} [D]_{1,2} \right\} q dz
 \end{aligned}$$

$$\tau_{xz}^k = q \left\{ \begin{array}{l} \sum_{i=1}^k [Q^i]_{1,2} [B]_{1,2} (z_{k+1} - z_k) \\ + R_x \cos \theta \sum_{i=1}^k [Q^i]_{1,2} [D]_{1,2} (z_{k+1} - z_k) \\ + \frac{1}{2} \cos \theta \sum_{i=1}^k [Q^i]_{1,2} [D]_{1,2} (z_{k+1}^2 - z_k^2) \end{array} \right\} \quad (20)$$

3. Results and Discussion

The present analysis has been discussed based on the axial in-plane and inter-laminar shear stresses distribution of tapered laminated cantilever beam subjected to different combination of moistures and temperatures. Based on the above formulations a complete MATLAB code has been developed and validated. Various results for different fiber orientations and stacking sequences (*viz.* symmetric and anti-symmetric laminates) have also been obtained and presented in the following subsections.

3.1. Validation of Developed MATLAB Code

In order to verify the developed code the dimensions and mechanical properties considered for carbon/epoxy (AS4/3501-6) rectangular laminated cantilever beam are presented in [15]. Fig. 2 shows the inter-laminar shear stresses distribution of this beam under thermal environment. It has been observed that result from the present code is excellent agreement with the already published results of Su [15] in case of thermal loading.

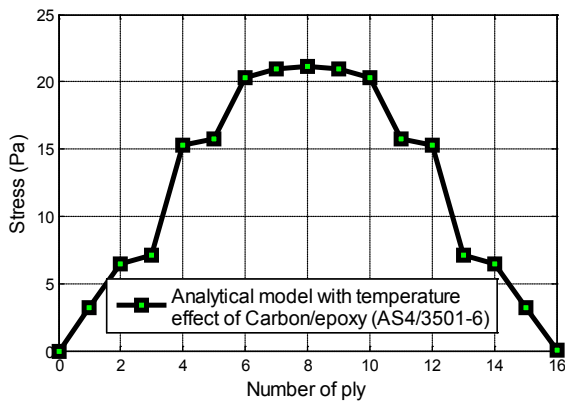


Figure 2. Inter-laminar shear stress distribution for beam

Three different types of laminates with sixteen layered (such as carbon/epoxy (AS4/3501-6), Kevlar/epoxy (Aramid 149/epoxy) and graphite/epoxy (GY-70/934)) have been considered for the analysis of tapered circular laminated cantilever beam having radius of 0.013m and thickness (t_{ply}) of each ply is 0.001321m. The material properties used are available in [4]. In the present analysis, the stacking sequence of laminate considered is $[5/90/0/90/0/5]_s$.

The variations of inter-laminar shear stresses across the thickness of the tapered circular graphite/epoxy beam at different cross sections are depicted in Fig. 3. It is clearly

observed from Fig. 3 that the inter-laminar stresses have a significant effect on the cross sections of tapered composite beam.

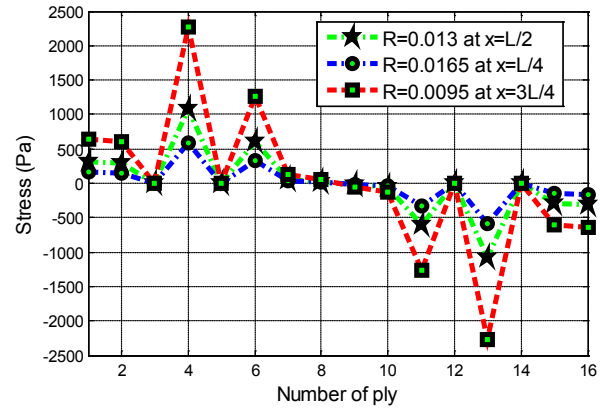


Figure 3. Interlaminar shear stress distribution of tapered beam

The Fig. 4 shows that the normalized axial stress distribution of tapered laminated cantilever beam considering different composite materials with $t_{ply}=0.001321m$, $R=0.0130m$, $\Delta T=325K$ and $\Delta C=1$. It is also observed from Fig. 4 that the normalized stress is more pronounced for graphite/epoxy laminated beam.

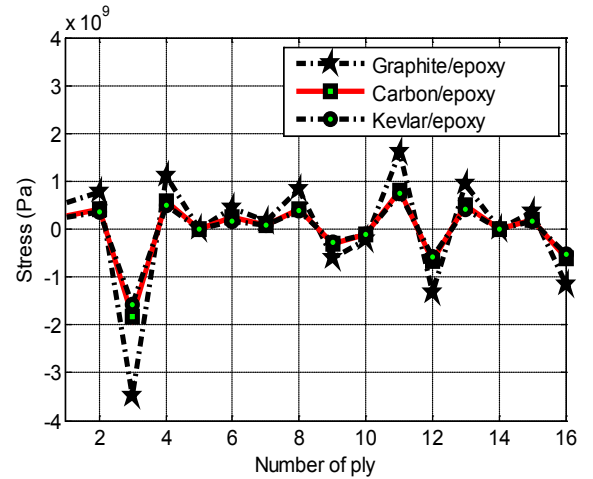


Figure 4. Normalized σ_x stress distribution of tapered beam

The normalized axial stress distribution for tapered graphite/epoxy laminated cantilever beam with different combinations of moisture concentrations and constant temperature ($0 K$) is shown in Fig. 5. It has been observed from Fig. 5 that the moisture concentrations have a significant effect on the axial stress distribution.

The Fig. 6 shows the normalized stress distribution (σ_x) of tapered beam having different types of stacking sequences with $t_{ply}=0.001321m$, $R=0.0130m$, $\Delta T=325K$ and $\Delta C=1$. It is clearly observed that the induced stress is more in case of anti-symmetric laminate. The comparison of increased stress in 0° ply due to hygro-thermal loading is presented in Table 1. From the Table 1, it is observed that the fiber orientation of the tapered laminated beam plays an important role in the variations of hygro-thermal induced stresses and it is also

cleared that the constituent of 0° and 90° plies demonstrates the greatest significant due to hygro-thermal effect.

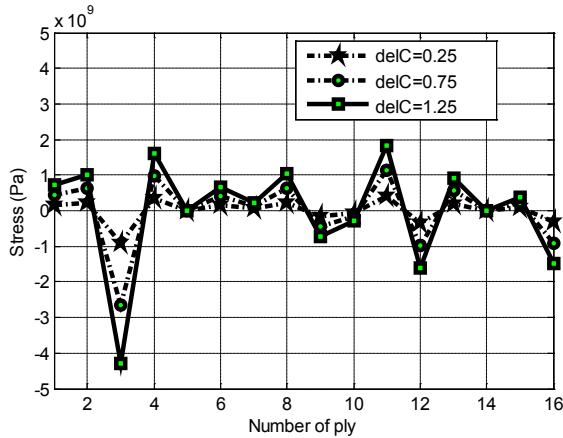


Figure 5. Normalized σ_x stress distribution with different moisture concentrations and Constant temperature

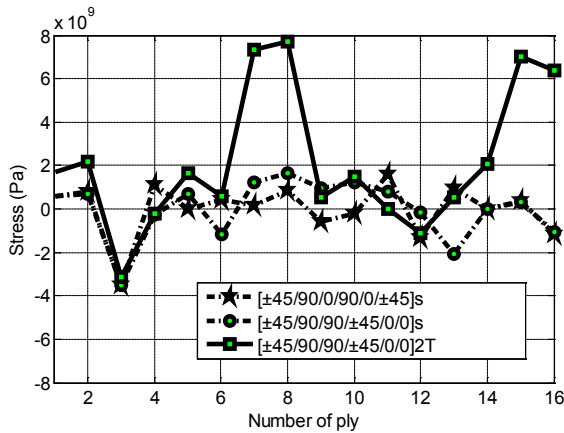


Figure 6. Normalized σ_x distribution for different stacking sequences for graphite/epoxy tapered beam

Table 1. Comparisons of increased stress in 0° ply

| Stacking sequence | Max. σ_x (MPa) due to hygro and thermal loadings | Max. σ_x (MPa) due to thermal loading | Increased σ_x (MPa) due to hygro loading |
|----------------------|---|--|---|
| | 0° | 0° | 0° |
| [±45/90/0/90/0/±45]S | 933.6 | 204.8 | 728.8 |
| [±45/90/2/±45/0/2]S | 1657.0 | 113.76 | 1543.4 |

4. Conclusions

An analytical method has been modified in order to predict the stress distribution within the layers and interfaces of circular tapered laminated beam under distributed, hygro and thermal loadings. From the present study, the following important conclusions may be made

- a) The axial in-plane stresses increases with the increases of moisture concentrations and temperatures.
- b) The combinations of different moisture concentrations and constant temperature have a significant effect on the axial in-plane stresses compared to the combination of different temperatures and constant moisture concentration.
- c) The fiber orientation of the plies plays an important role on the hygro-thermally induced axial in-plane stresses. This is mainly caused by the hygro-thermal induced moments which occur due to the mismatch of coefficients of axial thermal expansion and moisture expansion in each ply of the laminate

APPENDIX

Transformations of Stiffness Matrix

Stress and Strain Transformation Matrices: For plane stress condition, 2D stress and Strain transformation matrix rotated a positive angle θ about x-axis can be written as,

$$[T_\sigma(\theta)]_x = \begin{bmatrix} 1 & 0 & 0 \\ 0 & m_x^2 & 0 \\ 0 & 0 & m_x \end{bmatrix} \text{ and } [T_\epsilon(\theta)]_x = \begin{bmatrix} 1 & 0 & 0 \\ 0 & m_x^2 & 0 \\ 0 & 0 & m_x \end{bmatrix}$$

For plane stress condition, the 2D stress transformation matrix rotated a positive angle ϕ about z-axis can be obtained as,

$$[T_{\sigma \text{ or } \epsilon}(\phi)]_z = \begin{bmatrix} m_z^2 & n_z^2 & 2m_z n_z \\ n_z^2 & m_z^2 & -2m_z n_z \\ -m_z n_z & m_z n_z & m_z^2 - n_z^2 \end{bmatrix}$$

Where, $m_x = \cos \theta$, $m_z = \cos \phi$ and $n_z = \sin \phi$. Now, general transformation equation of stiffness matrix from material to laminate coordinate system can be written as, $[\bar{Q}] = [T_\sigma]^{-1} [Q] [T_\epsilon]$ Where, $[Q]$ and $[\bar{Q}]$ are the reduced stiffness matrices

of lamina which represent the stress/strain relationship with respect to material (1-2) coordinate system and laminate (x-y) coordinate system, respectively.

Transformation of CTE and CME: $[\alpha]_{x,y} = [T_\varepsilon]_z^{-1} [T_\varepsilon]_x^{-1} [\alpha]_{1,2}$, $[\beta]_{x,y} = [T_\varepsilon]_z^{-1} [T_\varepsilon]_x^{-1} [\beta]_{1,2}$

$$\begin{aligned}\alpha_x &= m_z^2 \alpha_1 + m_x^2 n_z^2 \alpha_2 & \beta_x &= m_z^2 \beta_1 + m_x^2 n_z^2 \beta_2 \\ \alpha_x &= n_z^2 \alpha_1 + m_x^2 m_z^2 \alpha_2 & \text{and } \beta_x &= n_z^2 \beta_1 + m_x^2 m_z^2 \beta_2 \\ \alpha_{xy} &= 2m_z n_z (\alpha_1 - m_x^2 \alpha_2) & \beta_{xy} &= 2m_z n_z (\beta_1 - m_x^2 \beta_2)\end{aligned}$$

Transformation of stiffness matrix for the lamina that first rotated θ about x-axis, then about ϕ about z-axis can be written as,

$$\begin{aligned}\overline{Q_{11}} &= m_z^4 Q_{11} + 2m_z^2 n_z^2 (m_x^2 Q_{12} + 2m_x^2 Q_{66}) + m_x^4 n_z^4 Q_{22} \\ \overline{Q_{12}} &= m_z^2 n_z^2 (Q_{11} + m_x^4 Q_{22} - 4m_x^2 Q_{66}) + (m_z^4 + n_z^4) m_x^2 Q_{12} \\ \overline{Q_{22}} &= n_z^4 Q_{11} + 2m_z^2 n_z^2 (m_x^2 Q_{12} + 2m_x^2 Q_{66}) + m_z^4 m_x^2 Q_{22} \\ \overline{Q_{16}} &= m_z^3 n_z (Q_{11} - m_x^2 Q_{12} - 2m_x^2 Q_{66}) + m_z n_z^3 (m_x^2 Q_{12} - m_x^4 Q_{22} + 2m_x^2 Q_{66}) \\ \overline{Q_{26}} &= m_z n_z^3 (Q_{11} - m_x^2 Q_{12} - 2m_x^2 Q_{66}) + m_z^3 n_z (m_x^2 Q_{12} - m_x^4 Q_{22} + 2m_x^2 Q_{66}) \\ \overline{Q_{66}} &= m_z^2 n_z^2 (Q_{11} + m_x^4 Q_{22} - 2m_x^2 Q_{12} - 2m_x^2 Q_{66}) + (m_z^4 + n_z^4) m_x^2 Q_{66}\end{aligned}$$

Total Extensional, Coupling and Bending Stiffness Matrices are,

$$\begin{aligned}\overline{[A_{11}]} &= 2\pi R_x \sum_{n=1}^k \left[m_z^4 Q_{11} + m_z^2 n_z^2 (Q_{12} + 2Q_{66}) + \frac{3}{8} n_z^4 Q_{22} \right] (z'_{k+1} - z'_k) \\ \overline{[A_{12}]} &= 2\pi R_x \sum_{n=1}^k \left[m_z^2 n_z^2 (Q_{11} + \frac{3}{8} Q_{22} - 2Q_{66}) + \frac{1}{2} (m_z^4 + n_z^4) Q_{12} \right] (z'_{k+1} - z'_k) \\ \overline{[A_{22}]} &= 2\pi R_x \sum_{n=1}^k \left[n_z^4 Q_{11} + m_z^2 n_z^2 (Q_{12} + 2Q_{66}) + \frac{3}{8} m_z^4 Q_{22} \right] (z'_{k+1} - z'_k) \\ \overline{[A_{16}]} &= 2\pi R_x \sum_{n=1}^k \left[m_z^3 n_z (Q_{11} - \frac{1}{2} Q_{12} - Q_{66}) + m_z n_z^3 (\frac{1}{2} Q_{12} - \frac{3}{8} Q_{22} + Q_{66}) \right] (z'_{k+1} - z'_k) \\ \overline{[A_{26}]} &= 2\pi R_x \sum_{n=1}^k \sum_{n=1}^k \left[m_z n_z^3 (Q_{11} - \frac{1}{2} Q_{12} - Q_{66}) + m_z^3 n_z (\frac{1}{2} Q_{12} - \frac{3}{8} Q_{22} + Q_{66}) \right] (z'_{k+1} - z'_k) \\ \overline{[A_{66}]} &= 2\pi R_x \sum_{n=1}^k \left[m_z^2 n_z^2 (Q_{11} + \frac{3}{8} Q_{22} - Q_{12} - Q_{66}) + \frac{1}{2} (m_z^4 + n_z^4) Q_{66} \right] (z'_{k+1} - z'_k) \\ \overline{[B_{11}]} &= \pi R_x \sum_{n=1}^k \left[m_z^4 Q_{11} + m_z^2 n_z^2 (Q_{12} + 2Q_{66}) + \frac{3}{8} n_z^4 Q_{22} \right] (z'^2_{k+1} - z'^2_k) \\ \overline{[B_{12}]} &= \pi R_x \sum_{n=1}^k \left[m_z^2 n_z^2 (Q_{11} + \frac{3}{8} Q_{22} - 2Q_{66}) + \frac{1}{2} (m_z^4 + n_z^4) Q_{12} \right] (z'^2_{k+1} - z'^2_k) \\ \overline{[B_{22}]} &= \pi R_x \sum_{n=1}^k \left[n_z^4 Q_{11} + m_z^2 n_z^2 (Q_{12} + 2Q_{66}) + \frac{3}{8} m_z^4 Q_{22} \right] (z'^2_{k+1} - z'^2_k)\end{aligned}$$

$$\begin{aligned}
\overline{[B_{16}]} &= \pi R_x \sum_{n=1}^k \left[m_z^3 n_z (Q_{11} - \frac{1}{2} Q_{12} - Q_{66}) + m_z n_z^3 (\frac{1}{2} Q_{12} - \frac{3}{8} Q_{22} + Q_{66}) \right] (z'_{k+1}{}^2 - z'_k{}^2) \\
\overline{[B_{26}]} &= \pi R_x \sum_{n=1}^k \left[m_z n_z^3 (Q_{11} - \frac{1}{2} Q_{12} - Q_{66}) + m_z^3 n_z (\frac{1}{2} Q_{12} - \frac{3}{8} Q_{22} + Q_{66}) \right] (z'_{k+1}{}^2 - z'_k{}^2) \\
\overline{[B_{66}]} &= \pi R_x \sum_{n=1}^k \left[m_z^2 n_z^2 (Q_{11} + \frac{3}{8} Q_{22} - Q_{12} - Q_{66}) + \frac{1}{2} (m_z^4 + n_z^4) Q_{66} \right] (z'_{k+1}{}^2 - z'_k{}^2) \\
\overline{[D_{11}]} &= \frac{2\pi R_x}{3} \sum_{n=1}^k \left[m_z^4 Q_{11} + m_z^2 n_z^2 (Q_{12} + 2Q_{66}) + \frac{3}{8} n_z^4 Q_{22} \right] (z'_{k+1}{}^3 - z'_k{}^3) \\
&\quad + 2\pi R_x^3 \sum_{n=1}^k \left[\frac{1}{2} m_z^4 Q_{11} + \frac{3}{4} m_z^2 n_z^2 (Q_{12} + 2Q_{66}) + \frac{5}{16} n_z^4 Q_{22} \right] (z'_{k+1} - z'_k) \\
\overline{[D_{12}]} &= \frac{2\pi R_x}{3} \sum_{n=1}^k \left[m_z^2 n_z^2 (Q_{11} + \frac{3}{8} Q_{22} - 2Q_{66}) + \frac{1}{2} (m_z^4 + n_z^4) Q_{12} \right] (z'_{k+1}{}^3 - z'_k{}^3) \\
&\quad + 2\pi R_x^3 \sum_{n=1}^k \left[m_z^2 n_z^2 (\frac{1}{2} Q_{11} + \frac{5}{16} Q_{22} - \frac{3}{2} Q_{66}) + \frac{3}{8} (m_z^4 + n_z^4) Q_{12} \right] (z'_{k+1} - z'_k) \\
\overline{[D_{22}]} &= \frac{2\pi R_x}{3} \sum_{n=1}^k \left[n_z^4 Q_{11} + m_z^2 n_z^2 (Q_{12} + 2Q_{66}) + \frac{3}{8} m_z^4 Q_{22} \right] (z'_{k+1}{}^3 - z'_k{}^3) \\
&\quad + 2\pi R_x^3 \sum_{n=1}^k \left[\frac{1}{2} n_z^4 Q_{11} + \frac{3}{4} m_z^2 n_z^2 (Q_{12} + 2Q_{66}) + \frac{5}{16} m_z^4 Q_{22} \right] (z'_{k+1} - z'_k) \\
\overline{[D_{16}]} &= \frac{2\pi R_x}{3} \sum_{n=1}^k \left[\begin{array}{l} m_z^3 n_z (Q_{11} - \frac{1}{2} Q_{12} - Q_{66}) \\ + m_z n_z^3 (\frac{1}{2} Q_{12} - \frac{3}{8} Q_{22} + Q_{66}) \end{array} \right] (z'_{k+1}{}^3 - z'_k{}^3) \\
&\quad + 2\pi R_x^3 \sum_{n=1}^k \left[\begin{array}{l} m_z^3 n_z (\frac{1}{2} Q_{11} - \frac{3}{8} Q_{12} - \frac{3}{4} Q_{66}) \\ + m_z n_z^3 (\frac{3}{8} Q_{12} - \frac{5}{16} Q_{22} + \frac{3}{4} Q_{66}) \end{array} \right] (z'_{k+1} - z'_k) \\
\overline{[D_{26}]} &= \frac{2\pi R_x}{3} \sum_{n=1}^k \left[\begin{array}{l} m_z n_z^3 (Q_{11} - \frac{1}{2} Q_{12} - Q_{66}) \\ + m_z^3 n_z (\frac{1}{2} Q_{12} - \frac{3}{8} Q_{22} + Q_{66}) \end{array} \right] (z'_{k+1}{}^3 - z'_k{}^3) \\
&\quad + 2\pi R_x^3 \sum_{n=1}^k \left[\begin{array}{l} m_z n_z^3 (\frac{1}{2} Q_{11} - \frac{3}{8} Q_{12} - \frac{3}{4} Q_{66}) \\ + m_z^3 n_z (\frac{3}{8} Q_{12} - \frac{5}{16} Q_{22} + \frac{3}{4} Q_{66}) \end{array} \right] (z'_{k+1} - z'_k) \\
\overline{[D_{66}]} &= \frac{2\pi R_x}{3} \sum_{n=1}^k \left[m_z^2 n_z^2 (Q_{11} + \frac{3}{8} Q_{22} - Q_{12} - Q_{66}) + \frac{1}{2} (m_z^4 + n_z^4) Q_{66} \right] (z'_{k+1}{}^3 - z'_k{}^3) \\
&\quad + 2\pi R_x^3 \sum_{n=1}^k \left[m_z^2 n_z^2 (\frac{1}{2} Q_{11} + \frac{5}{16} Q_{22} - \frac{3}{4} Q_{12} - \frac{3}{4} Q_{66}) + \frac{3}{8} (m_z^4 + n_z^4) Q_{66} \right] (z'_{k+1} - z'_k)
\end{aligned}$$

Overall Hygro-Thermal Induced Force and Moment of the tapered Beam:

$$\begin{aligned}
[\overline{N}]_x^{HT} &= \int_0^{2\pi} [N]_x^{HT} R_x d\theta \\
&= \pi R_x (\Delta T + \Delta C) \left[\begin{array}{l} \left(m_z^6 + m_z^2 n_z^4 + 2m_z^4 n_z^2 \right) \left\{ \begin{array}{l} 2Q_{11}(\alpha_1 + \beta_1) \\ + \frac{3}{4} Q_{12}(\alpha_2 + \beta_2) \end{array} \right\} \\ + \left(n_z^6 + m_z^4 n_z^2 + 2m_z^2 n_z^4 \right) \left\{ \begin{array}{l} Q_{12}(\alpha_1 + \beta_1) \\ + \frac{5}{8} Q_{22}(\alpha_2 + \beta_2) \end{array} \right\} \end{array} \right] (z'_{k+1} - z'_k) \\
[\overline{N}]_y^{HT} &= \int_0^{2\pi} [N]_y^{HT} R_x d\theta \\
&= \pi R_x (\Delta T + \Delta C) \left[\begin{array}{l} \left(n_z^6 + m_z^4 n_z^2 + 2m_z^2 n_z^4 \right) \left\{ 2Q_{11}(\alpha_1 + \beta_1) + \frac{3}{4} Q_{12}(\alpha_2 + \beta_2) \right\} \\ + \left(m_z^6 + m_z^2 n_z^4 + 2m_z^4 n_z^2 \right) \left\{ Q_{12}(\alpha_1 + \beta_1) + \frac{5}{8} Q_{22}(\alpha_2 + \beta_2) \right\} \end{array} \right] (z'_{k+1} - z'_k) \\
[\overline{N}]_{xy}^{HT} &= \int_0^{2\pi} [N]_{xy}^{HT} R_x d\theta \\
&= \pi R_x (\Delta T + \Delta C) \left[\begin{array}{l} \left(m_z^5 n_z + m_z n_z^5 \right) \left\{ \begin{array}{l} (2Q_{11} - Q_{12})(\alpha_1 + \beta_1) \\ + \left(\frac{3}{4} Q_{12} - \frac{5}{8} Q_{22} \right) (\alpha_2 + \beta_2) \end{array} \right\} \\ + 2m_z^3 n_z^3 \end{array} \right] (z'_{k+1} - z'_k) \\
[\overline{M}]_x^{HT} &= \int_0^{2\pi} [M]_x^{HT} R_x d\theta \\
&= \frac{\pi R_x (\Delta T + \Delta C)}{2} \left[\begin{array}{l} \left(m_z^6 + m_z^2 n_z^4 + 2m_z^4 n_z^2 \right) \left\{ 2Q_{11}(\alpha_1 + \beta_1) + \frac{3}{4} Q_{12}(\alpha_2 + \beta_2) \right\} \\ + \left(n_z^6 + m_z^4 n_z^2 + 2m_z^2 n_z^4 \right) \left\{ Q_{12}(\alpha_1 + \beta_1) + \frac{5}{8} Q_{22}(\alpha_2 + \beta_2) \right\} \end{array} \right] (z'^2_{k+1} - z'^2_k) \\
[\overline{M}]_y^{HT} &= \int_0^{2\pi} [M]_y^{HT} R_x d\theta \\
&= \frac{\pi R_x (\Delta T + \Delta C)}{2} \left[\begin{array}{l} \left(n_z^6 + m_z^4 n_z^2 + 2m_z^2 n_z^4 \right) \left\{ 2Q_{11}(\alpha_1 + \beta_1) + \frac{3}{4} Q_{12}(\alpha_2 + \beta_2) \right\} \\ + \left(m_z^6 + m_z^2 n_z^4 + 2m_z^4 n_z^2 \right) \left\{ Q_{12}(\alpha_1 + \beta_1) + \frac{5}{8} Q_{22}(\alpha_2 + \beta_2) \right\} \end{array} \right] (z'^2_{k+1} - z'^2_k) \\
[\overline{M}]_{xy}^{HT} &= \int_0^{2\pi} [M]_{xy}^{HT} R_x d\theta \\
&= \frac{\pi R_x (\Delta T + \Delta C)}{2} \left[\begin{array}{l} \left(m_z^5 n_z + m_z n_z^5 \right) \left\{ \begin{array}{l} (2Q_{11} - Q_{12})(\alpha_1 + \beta_1) \\ + \left(\frac{3}{4} Q_{12} - \frac{5}{8} Q_{22} \right) (\alpha_2 + \beta_2) \end{array} \right\} \\ + 2m_z^3 n_z^3 \end{array} \right] (z'^2_{k+1} - z'^2_k)
\end{aligned}$$

REFERENCES

- [1] J. M. Whitney and J. E. Ashton, Effect of environment on the elastic response of layered composite plates, *Journal of AIAA*, vol. 9 (9), pp. 1708–1713, 1971.
- [2] R. B. Pipes, J. R. Vinson and T. W. Chou, On the hygrothermal response of laminated composite systems, *Journal of Composite Materials*, vol. 10, pp. 129–148, 1976.
- [3] D. F. Sims and H. E. Wilson, Distribution of shearing stresses in a composite beam under transverse loading, *Journal of Composites*, pp. 185–191, 1978.
- [4] K. S. Sai Ram and P. K. Sinha, Hygrothermal effects on the bending characteristics of laminated composite plate. *Int. Journal of computers and structures*, vol. 40(4), pp. 1009–1015, 1991.
- [5] K. S. Sai Ram and P. K. Sinha, Hygrothermal effects on the free vibration of laminated composite plate. *Journal of sound and vibration*, vol. 158(1), pp. 133–148, 1992.
- [6] K. S. Sai Ram and P. K. Sinha, Hygrothermal effects on the buckling of laminated composite plate. *Journal of composite structures*, vol. 21, pp. 233–247, 1992.
- [7] W. S. Chan and K. C. Demirhan, A simple closed form solution of bending stiffness for laminated composite tube, *Journal of Reinforced Plastics and Composites*, vol. 19(04), pp. 278–291, 2000.
- [8] J. Q. Tarn and Y. M. Wang, Laminated composite tubes under extension, torsion, bending, shearing and pressuring: a state space approach, *Int. Journal of Solids and structures*, vol. 38, pp. 9053–9075, 2001.
- [9] B. P. Patel, M. Ganapathi and D. P. Makhecha, Hygrothermal effects on the structural behavior of thick composite laminated using higher order theory, *Journal of composite structures*, vol. 56, pp. 25–34, 2002.
- [10] A. M. Zenkour, Analytical solution for bending of cross-ply laminated plates under thermo-mechanical loading, *Journal of composite structures*, vol. 65, pp. 367–379, 2004.
- [11] N. V. S. Naidu and P. K. Sinha, Nonlinear finite element analysis of laminated composites shells in hygrothermal environment, *Journal of composites structures*, vol. 69, pp. 387–395, 2005.
- [12] X. Wang, K. Dong and X. Y. Wang, Hygrothermal effect on dynamic inter-laminar stresses in laminated plates with piezoelectric actuators, *Journal of composite structures*, vol. 71, pp. 220–228, 2005.
- [13] N. V. S. Naidu and P. K. Sinha, Nonlinear Free vibration analysis of laminated composite shells in hygrothermal environments, *Journal of composite structures*, vol. 77, pp. 475–483, 2007.
- [14] A. Bahrami, and A. Nosier, Inter-laminar hygrothermal stresses in laminated plates, *Int. Journal of solids and structures*, vol. 44, pp. 8119–8142, 2007.
- [15] C. W. Su, Thermal Stresses of composite beams with rectangular and tubular cross-sections, M.S. Thesis, University of Texas at Arlington, 2007.
- [16] C. S. Rao, Analysis of Tapered Laminated Composite Tubes under Tension and Torsion, M.S. Thesis, University of Texas at Arlington, 2007.
- [17] Z. S. Shao, and G. W. Ma, Thermo-mechanical stresses in functionally graded circular hollow cylinder with linearly increasing boundary temperature, *Journal of Composite Structures*, vol. 83, pp. 259–265, 2008.
- [18] K. A. Syed, C. W. Su and W. S. Chan, Analysis of fiber-reinforced composite beams under temperature environment, *Journal of Thermal Stresses*, vol. 32, pp. 311–321, 2009.
- [19] A. M. Zenkour, Hygro-thermo-mechanical effect on FGM plates resting on elastic foundations, *Journal of Composite Structures*, vol. 93, pp. 234–238, 2010.
- [20] S. K. Singh and A. Chakrabarti, Hygrothermal analysis of laminated composite plates by using efficient higher order shear deformation theory, *Journal of Solid Mechanics*, vol. 3(1), pp. 85–95, 2011.
- [21] I. M., Daniel and O. Shai, *Engineering mechanics of composite materials*, Oxford University Press, New York, 1994.
- [22] R. M. Jones, *Mechanics of composite materials*, Second Edition, Tata McGraw Hill, 1999.